Using Model Substrates To Study the Dependence of Focal Adhesion Formation on the Affinity of Integrin−Ligand Complexes†

Mihoko Kato‡ and Milan Mrksich*

Department of Chemistry, Institute of Biophysical Dynamics, The University of Chicago, Chicago, Illinois 60637

Received July 18, 2003; Revised Manuscript Received November 25, 2003

ABSTRACT: The adhesion of mammalian cells is mediated by the binding of cell-surface integrin receptors to peptide ligands from the extracellular matrix and the clustering of these receptors into focal adhesion complexes. This paper examines the effect of one mechanistic variable, ligand affinity, on the assembly of focal adhesions (FAs) in order to gain mechanistic insight into this process. This study uses self-assembled monolayers of alkanethiolates on gold as a substrate to present either a linear or cyclic Arg-Gly-Asp peptide at identical densities. Inhibition assays showed that the immobilized cyclic RGD is a higher affinity ligand than linear RGD. 3T3 Swiss fibroblasts attached to substrates presenting the cyclic peptide at twice the rate they attached to substrates presenting the linear peptide. Quantitation of focal adhesions revealed that cells on cyclic RGD had twice the number of FAs as did cells on linear RGD and that these focal adhesions were on average smaller. These findings show that affinity affects the assembly of integrins into focal adhesions and support a model based on competing rates of nucleation and growth of FAs to explain the change in distribution of FAs with ligand affinity. This study is important because it provides a model system that is well-suited for biophysical studies of integrin-mediated cell adhesion and reveals insight into one mechanism utilized by cells to perceive environmental changes.

Most mammalian cells are adherent and must attach and spread on a protein matrix in order to proliferate, differentiate, and maintain normal metabolic activities (*1*−*3*). This extracellular matrix (ECM)[1] comprises an insoluble network of fibrous proteins and polysaccharides that serves as a structural scaffold to which cells adhere (by way of receptor−ligand complexes) and provides numerous signaling molecules that regulate cell behavior. While cell−matrix interactions are an important theme in cell biology, studies that aim to elucidate the roles played by discrete ligands and receptors are intrinsically difficult, in part because it is not straightforward to control the composition of ligands on the substrate and in part because cells can remodel the surfaces to which they are attached to introduce other ligand−receptor interactions (*4*, *5*). Model substrates that can unambiguously control the receptor−ligand interactions between an adherent cell and substrate now provide new opportunities for mechanistic studies of cell adhesion (*6*, *7*).

Cell adhesion requires the interplay of structural and signaling components which together allow the cell to attach, change morphology, and modulate behavior. Both components are largely regulated by the aggregation of adhesion receptors and other cellular proteins into focal adhesion complexes. A central component of focal adhesion complexes is integrins, a family of approximately 25 transmembrane receptors involved in bridging communication between the extracellular environment and the cytosol of the cell. The extracellular domain of this $\alpha\beta$ heterodimeric receptor binds peptide ligands of ECM proteins, such as Arg-Gly-Asp (RGD) in fibronectin. Upon ligand binding, the intracellular domain recruits cytosolic proteins which mediate signal transduction pathways and form mechanical links to the actin cytoskeleton of the cell. Through the engagement of integrin receptors, cells can adhere to the substrate, spread to assume a flattened morphology, and anchor the cytoskeleton to the substrate. In addition, cells can respond to environmental cues to determine cell survival, growth, and many aspects of subsequent behavior. Therefore, while signals from the environment affect individual ligand−receptor complexes, they are often deciphered at the level of focal adhesion complexes to determine subsequent cell behavior.

While the central role of the focal adhesion is clear, a mechanistic understanding of the process by which integrins assemble to give these structures is lacking. The rate of receptor clustering into focal adhesions is affected by characteristics of both the substrate and the cell and include diffusivity (a physical property of the membrane), the number of receptors expressed by the cell, the density of ligands, and the affinity of the receptor for the ligand (*8*). Because cells use a combination of these mechanisms to control behavior, understanding the effect of each variable on focal adhesion formation is an important link to understanding how external cues are integrated into cellular responses. Here we address the role that affinity of integrin−ligand interactions plays in focal adhesion formation.

† Funded by the National Institutes of Health (Grant GM 63116).

*To whom correspondence should be addressed: e-mail, mmrksich@midway.uchicago.edu.

‡ Present address: HHMI and Division of Biology, California Institute of Technology, Pasadena, CA 91125.

[1] Abbreviations: ECM, extracellular matrix; RGD, Arg-Gly-Asp; SAMs, self-assembled monolayers; GRGDS, Gly-Arg-Gly-Asp-Ser-NH_2; RGD*f*K, cyclic peptide Arg-Gly-Asp-DPhe-Lys; Cp-CO_2H, cyclopentadienyl acetic acid; Cp, cyclopentadiene; FAs, focal adhesions; FAK, focal adhesion kinase; MAPK, mitogen-activated protein kinase; THF, tetrahydrofuran; BSA, bovine serum albumin; PBS, phosphate-buffered saline; FITC, fluorescein isothiocyanate; TBST, Tris-buffered saline and 0.1% Tween; HRP, horseradish peroxidase.

10.1021/bi0352670 CCC: $27.50
Published on Web 02/18/2004

One of the challenges in studying the effects of the environment on focal adhesion formation is the design of surfaces that are molecularly well-defined and can be systematically varied. Because focal adhesion formation will depend on both the affinity and density of immobilized peptide, it is imperative that substrates that present either a high- or a low-affinity ligand do so at a strictly constant density (*9*). We used self-assembled monolayers (SAMs) of alkanethiolates on gold that present peptide ligands mixed among tri(ethylene glycol) groups because these substrates have several characteristics that make them well-suited for cell adhesion studies. First, the oligo(ethylene glycol) groups prevent nonspecific adsorption of proteins (*10*−*13*). This property ensures that cells can only attach by way of receptor interactions with immobilized peptides. Second, the surfaces are well ordered and present ligands in a homogeneous environment (*14*, *15*). Finally, it is possible to precisely control the density of an immobilized ligand by first preparing mixed SAMs from a ratio of two different alkanethiols in solution and following with a separate coupling reaction to introduce the ligands onto the surfaces.

We created surfaces that presented either a high- or a low-affinity RGD peptide at equal densities and found that the number, size, and distribution of focal adhesions within a cell are influenced by the affinity of the ligand for the integrin receptor. We propose a model based on relative rates of nucleation and growth of FAs to explain the influence of affinity on FA structure. We discuss the possibility that FAs are the functional unit which is affected by affinity and which in turn affects adhesion and migration of cells.

MATERIALS AND METHODS

Synthesis of Alkanethiols and Peptide Reagents. All amino acids and resins were purchased from Anaspec (San Jose, CA). Chemical reagents were purchased from Aldrich (St. Louis, MO). Linear GRGDS was synthesized using standard Fmoc solid-phase synthesis on an Fmoc-rink amide MHBA resin. Cyclic RGD*F*K was synthesized as described by Haubner et al. (*16*). Alkanethiols terminated in the hydroquinone group and the tri(ethylene glycol) group were prepared as described previously (*12*). The conjugates of peptide and cyclopentadiene were prepared by acylation of the α-amino group of the peptide Gly-Arg-Gly-Asp-Ser-NH_2 (GRGDS) or of the ϵ-amino group of lysine in the cyclic peptide Arg-Gly-Asp-DPhe-Lys (cRGD*F*K) with cyclopentadienyl acetic acid (Cp-CO_2H) to afford GRGDS-Cp or cRGD*F*K-Cp.

Cyclopentadienyl Ethyl Acetate (Cp-$CO_2CH_2CH_3$). A solution of ethyl chloroacetate (438 μL, 4.1 mmol) in THF (5 mL) was cooled to 0 °C and treated with dropwise addition of sodium cyclopentadiene (2 mL of 2 M solution in THF, 4 mmol). The mixture was allowed to warm to room temperature and stirred for 3 h. The reaction was quenched with water and extracted with CH_2Cl_2 (3 × 15 mL). The combined organic layers were dried over $MgSO_4$, filtered, and concentrated to afford an oil, which was then purified by flash chromatography with CH_2Cl_2 and hexanes (1:3) to afford the product: ^{1}H NMR δ ($CDCl_3$) 1.25 (m, 3H), 3.05 (d, J = 11.2 Hz, 2H), 3.50 (d, J = 11.8, 2H), 4.16 (m, 2H), 6.20−6.60 (m, 3H).

Cyclopentadienyl Acetic Acid (Cp-CO_2H). A solution of cyclopentadienyl ethyl acetate in dioxane (10 mL) with sodium hydroxide (12 N, 50% v/v) was stirred at room temperature for 45 min. The reaction was washed with CH_2Cl_2 (3 × 15 mL) and then acidified with 1 N HCl to a pH of 3.0. The aqueous phase was then extracted with CH_2Cl_2 (3 × 15 mL), dried over $MgSO_4$, and concentrated to afford the product: ^{1}H NMR δ ($CDCl_3$) 3.05 (d, J = 11.2 Hz, 2H), 3.57 (d, J = 11.8 Hz, 2H), 6.20−6.60 (m, 3H).

GRGDS-Cp or cRGDFK-Cp. A solution of cyclopentadienyl acetic acid (26 mg, 0.21 mmol) in THF (3 mL) was stirred with dicyclohexylcarbodiimide (67 mg, 0.32 mmol) and *N*-hydroxysuccinimide (37 mg, 0.32 mmol) at room temperature for 6 h. The mixture was filtered and added directly to free peptide, GRGDS or cRGD*F*K, in DMF and stirred overnight. The solution was concentrated and purified by a Sep-Pak C18 column (Waters, Milford, MA).

Preparation of Self-Assembled Monolayers. Substrates were prepared by evaporating titanium (40 Å) and then gold (150 Å) onto glass coverslips. These thin films of gold are transparent and compatible with optical and fluorescence microscopy techniques. We employed a method of monolayer preparation that ensured equivalent densities of ligand at the surface, regardless of the identity of the ligand. Self-assembled monolayers presenting approximately 4×10^{12} ligands/cm^2 were formed by immersing gold-coated substrates in an ethanolic solution that contained a mixture of the hydroquinone-terminated alkanethiol (10 μM) and the tri(ethylene glycol)-terminated alkanethiol (1 mM). The substrates were removed from solution after 6 h, washed with ethanol, and dried under a stream of nitrogen. The monolayers were immersed in an aqueous solution of benzoquinone for 2 min to convert the hydroquinone groups to the corresponding quinones. Peptides were immobilized by applying a drop of the diene−peptide conjugate in water (3 mM) to the substrates for 4 h. Cyclic voltammetry showed that the Diels−Alder reaction had gone to completion.

Cell Culture. 3T3 Swiss albino cells (ATCC) were cultured in Dulbecco's modified Eagle medium (DMEM; GIBCO-BRL, Carlsbad, CA) supplemented with 10% fetal bovine serum at 37 °C at 7.5% CO_2.

Focal Adhesion Imaging and Quantitation. Cells were plated on several identical monolayers presenting either linear or cyclic RGD and cultured at 37 °C in the presence of serum. Individual monolayers were removed from the culture at 6, 8, 10, 12, and 24 h after plating (one linear RGD and one cyclic RGD SAM), washed with PBS, and fixed in 3.7% paraformaldehyde for 4 min. The substrates were washed with PBS and then treated with 0.3% Triton X-100 in PBS for 1 min and blocking solution (1% BSA, 0.1% gelatin, and 0.1% Triton X-100 in PBS) for 30 min. To visualize focal adhesions, cells were treated with anti-vinculin antibody (Sigma, St. Louis, MO) diluted 1:400 in blocking solution for 1 h, followed by incubation with goat anti-mouse FITC antibody (Molecular Probes, Eugene, OR) at 1:400 dilution in blocking buffer for 1 h. Slides were washed three times with PBS containing 0.1% Triton X-100 between each antibody treatment. Substrates were mounted on glass slides and were viewed through a Zeiss microscope with image capture by a CCD camera with Openlab software (Improvision, Lexington, MA). FA size and spatial distribution were analyzed using IPLab, Scientific Imaging Software (Scanalytics, Fairfax, VA).

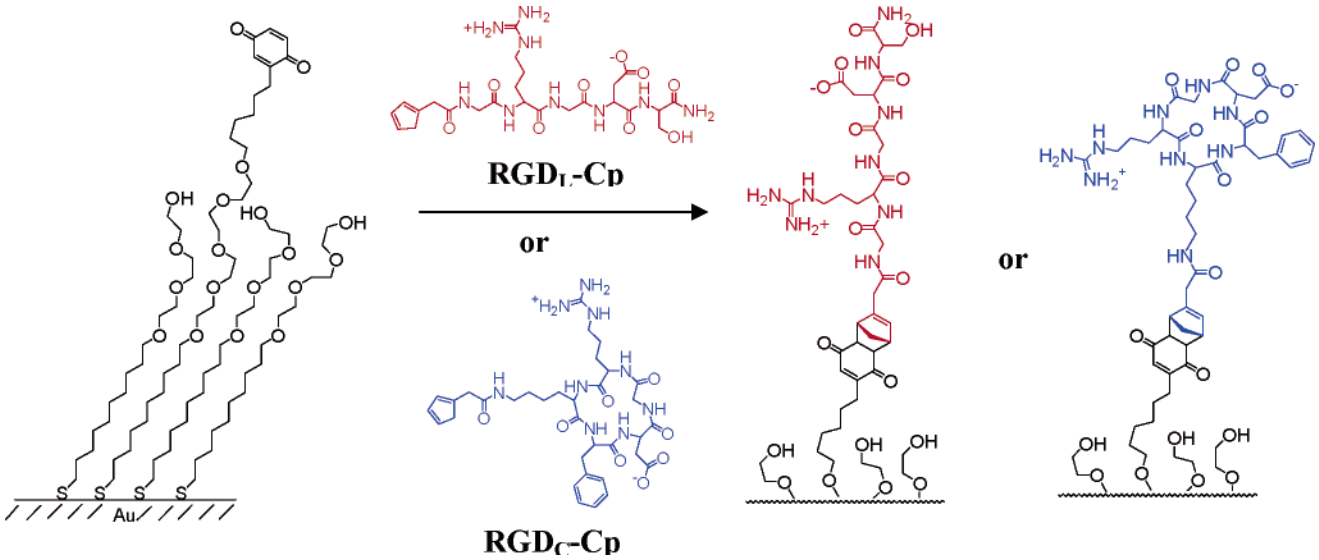

FIGURE 1: Monolayers presenting either the linear GRGDS or the cyclic RGD*F*K ligands were prepared by the Diels−Alder-mediated immobilization of peptide−diene conjugates to benzoquinone groups on the monolayer. Because the Diels−Alder reaction of cyclopentadiene with benzoquinone goes to completion, the density of peptide is determined by the density of the quinone-terminated alkanethiolate in the monolayer. This property ensures that monolayers presenting either the linear or cyclic ligand will maintain a constant density of ligand.

Inhibition Assay. Cells were harvested from cultureware with trypsin (0.25%)/ EDTA (0.53 mM). Separately, many samples of cells (20000 in 350 μL of media with serum) were incubated with soluble inhibitor (GRGDS or cRGD*F*K inhibitor) at concentrations ranging from 10 nM to 1 mM. After 3 min, the suspended cells were plated directly onto the SAMs. After the cells were incubated for 30 min at 37 °C, SAMs were transferred to a separate culture dish, and the number of cells was counted with an optical micrograph.

Assay of Focal Adhesion Signaling (Western Blotting). Cells were simultaneously plated on four linear RGD SAMs and four cyclic RGD SAMs in media supplemented with serum and kept at 37 °C. Individual substrates were removed 10, 20, 30, and 40 min after plating, washed with cold PBS, and treated with Laemmli's sample buffer (Bio-Rad, Hercules, CA) to lyse the cells. Lysates were boiled for 3 min and separated on a 7.5% SDS−polyacrylamide gel. Proteins were transferred to a nitrocellulose membrane, which was then blocked for 30 min in TBST (Tris-buffered saline and 0.1% Tween) containing 5% nonfat milk. The blot was incubated with anti-phosphoFAK antibody (Biosource, Camarillo, CA) (1:1000) in TBST overnight at 4 °C. The blot was incubated with goat anti-rabbit HRP antibody for 1 h and visualized using chemiluminescence (ECL kit; Amersham Biosciences, Piscataway, NJ) on Kodak film.

RESULTS

Preparation of Model Substrates. This work compares several aspects of cell adhesion on monolayers presenting peptides that are either a low-affinity or a high-affinity ligand for the cell-surface integrin receptors. For the low-affinity ligand, we used a linear pentapeptide containing the sequence Arg-Gly-Asp (RGD). We have previously shown that 3T3 Swiss fibroblasts attach efficiently to monolayers presenting this ligand and that the cells assemble focal adhesions and actin stress filaments (*9*, *17*). For the high-affinity ligand, we used a cyclic pentapeptide containing the RGD sequence. Kessler and co-workers have shown that soluble cyclized RGD peptide inhibits the attachment of cells at a 500−1000-fold lower concentration than does the corresponding linear peptide (*16*, *18*).

Because cell adhesion will depend on both the affinity and density of immobilized peptide (*9*), it is imperative that substrates that present either the high- or the low-affinity ligand do so at a strictly constant density. The common strategy with self-assembled monolayers for controlling the density of ligand, which relies on adjusting the ratio of two alkanethiols in the solution from which the monolayer is formed, has the limitation that the ratio of the alkanethiolates in the monolayer is never identical to that in the solution. Even when the densities of ligands in the monolayer are determined by independent measurement, the uncertainty in density can be as high as 30%. We therefore developed a strategy based on the Diels−Alder reaction to immobilize conjugates of the peptides and cyclopentadiene to the benzoquinone groups of a monolayer substrate (Figure 1) (*19*). First, mixed monolayers were prepared on optically transparent, gold-coated coverslips from a solution of mixed alkanethiols. Ninety-nine percent of the alkanethiols were terminated by a tri(ethylene glycol) group, which has previously been shown to almost completely prevent protein adsorption (*12*), and 1% was terminated by a hydroxyquinone group. The hydroxyquinone groups of the resulting monolayer were oxidized to the corresponding benzoquinone groups by a brief chemical treatment. The ligand was then immobilized to this surface through a quantitative Diels−Alder coupling between the benzoquinone groups of the monolayer and either cyclopentadiene-conjugated linear GRGDS or cyclic RGD*F*K. This strategy is well-suited for this task because the reaction is selective and proceeds in high yield, ensuring constant densities of ligand, even when different ligands are employed (*19*).

Cell Attachment to Model Substrates. We compared the attachment of 3T3 Swiss fibroblasts to monolayers presenting either the linear or cyclic RGD peptide with a control substrate having an adsorbed layer of fibronectin. A suspension of cells in serum-supplemented medium was added to culture dishes containing substrates. The cultures were kept

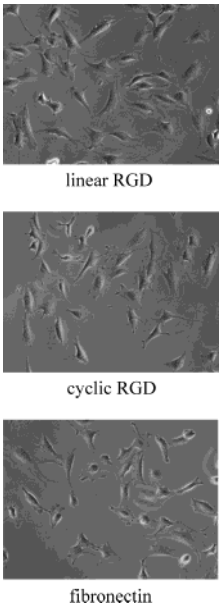

FIGURE 2: Optical micrographs of 3T3 Swiss albino fibroblasts attached after 12 h to monolayers presenting the linear RGD peptide (top), the cyclic RGD peptide (middle), or a methyl-terminated monolayer having an adsorbed layer of the extracellular matrix protein fibronectin (bottom). Cells spread well on all three substrates and proliferated to form a confluent monolayer when cultured in serum-supplemented medium.

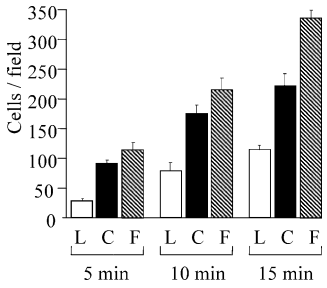

FIGURE 3: Comparison of the number of cells that attached to a monolayer presenting linear RGD (L), cyclic RGD (C), and fibronectin (F) at 5, 10, and 15 min after plating. Cells were counted in a field acquired through a 10× objective.

at 37 °C and examined periodically by optical microscopy. We found that cells attached efficiently to each of the three substrates (Figure 2). Quantitation of the rates of cell attachment to the substrates showed that attachment to cyclic RGD was approximately 2-fold faster than to linear RGD but that the rate of attachment was greatest on fibronectin-coated substrates (Figure 3). Moreover, cells assumed a similar spread morphology on each of three substrates. A control experiment verified that cells did not attach to monolayers presenting only tri(ethylene glycol) groups. The three substrates were fixed and stained with phalloidin−rhodamine after 16 h in culture to visualize actin stress filaments. There were no gross differences in the cytoskeletal structure of cells on the three substrates. These results establish that the model substrates are competent for studies of integrin-mediated cell adhesion.

Inhibition Assay. We determined the concentration of soluble peptide (either linear GRGDS or cyclic RGD*F*K) required to reduce, by one-half, the number of cells that attached to the model substrates. These inhibition experiments are important because they demonstrate that cell adhesion to the model substrates is biospecific (that is,

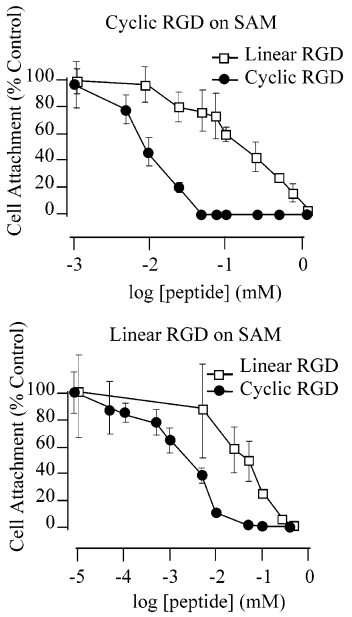

FIGURE 4: Plots showing the inhibition of cell attachment to the monolayer substrates by soluble peptides. The plot at the top shows data for the inhibition of cell attachment to monolayers presenting the cyclic peptide by both soluble linear and cyclic peptides. The plot at the bottom shows data for the inhibition of cell attachment to monolayers presenting the linear peptide by both soluble linear and cyclic peptides.

mediated only by integrin receptors binding to the peptide ligands) and because they provide estimates of the relative affinities of the linear and cyclic peptides for the integrin receptors. Suspended cells in medium (20000 cells/750 μL) were incubated for 5 min with either the linear or cyclic RGD peptide, at concentrations ranging from 10 nM to 1 mM, and then the cells were added directly onto monolayer substrates. For these experiments, we used substrates presenting lower densities of ligand (0.05% for linear RGD and 0.01% for cyclic RGD) because monomeric ligands are poor inhibitors of polyvalent adhesion. In both cases, the degree of inhibition increased with the concentration of soluble peptide, with complete inhibition at high concentrations of peptide (Figure 4). This result establishes that cell attachment is biospecific and that the monolayers prevent any secondary interactions between the cell and substrate. The concentration of soluble peptide that results in 50% attachment gives an estimate of the binding affinity between peptide and integrin (or multiple distinct integrins). For both model substrates (linear and cyclic RGD), the concentration of soluble linear peptide required to reduce attachment by one-half was approximately 22 times greater than that of soluble cyclic peptide. Hence, the cyclic peptide does indeed have higher affinity for the integrin receptors. The observation that either peptide can block cell attachment to both substrates reveals that the ligands are also bound by the same integrin receptor-(s).

Assembly and Distribution of Focal Adhesions. We next characterized the sizes and distributions of focal adhesions in cells adherent to substrates presenting linear or cyclic RGD to determine whether the aggregation of integrins into focal adhesions is dependent on the affinity of peptide ligands. Cells were allowed to attach to several substrates presenting either linear or cyclic RGD, always at a density of 1%, and were cultured in serum-supplemented medium. Independent

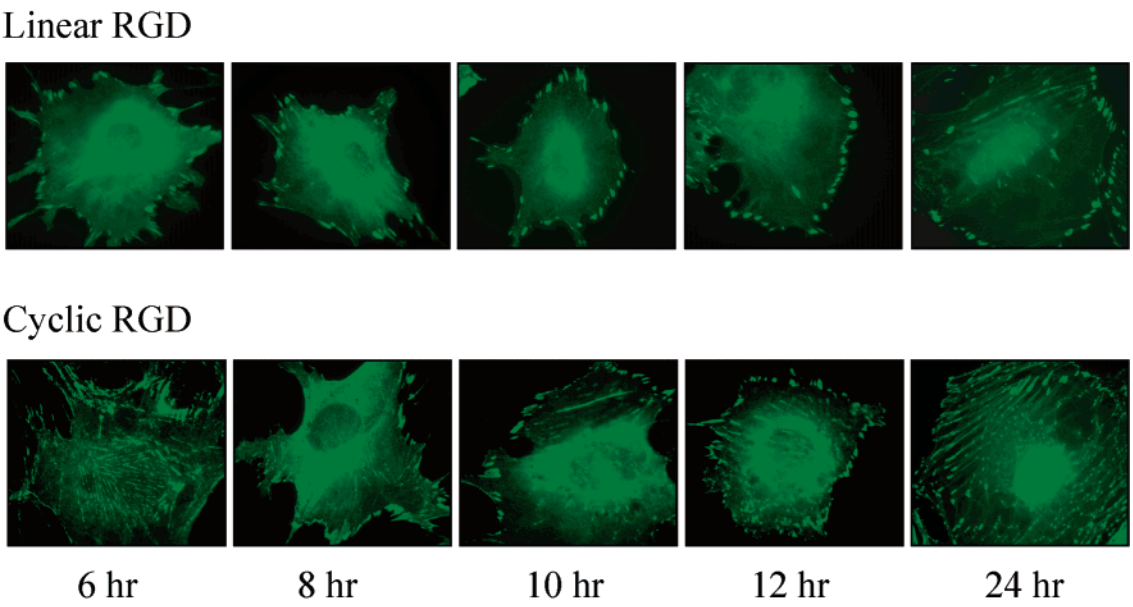

FIGURE 5: Time course of the evolution of focal adhesions in cells attached to monolayers presenting either linear or cyclic RGD peptide ligands. Fluorescent micrographs of representative cells that had been fixed and stained with anti-vinculin antibody are shown for 6, 8, 10, 12, and 24 h after attachment. Cells attached to linear RGD are characterized by focal adhesions that are larger and occur with greater frequency at the perimeter. Cells attached to cyclic RGD, by contrast, had smaller focal adhesions that were distributed more evenly throughout the cell.

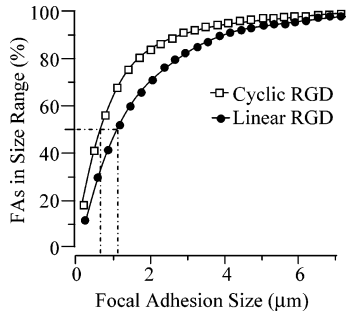

FIGURE 6: Probability curve of the size distribution of focal adhesions in cells adherent to cyclic and linear RGD SAMs. A total of 1386 and 726 focal adhesions were counted for cells on monolayers presenting cyclic RGD or linear RGD, respectively. Focal adhesions in cells on cyclic RGD were smaller (median = 0.78 μm^2) than focal adhesions in cells on linear RGD (median = 1.14 μm^2).

slides were removed from culture at times ranging from 6 to 24 h, fixed in paraformaldehyde, and stained with an antibody against vinculin and a secondary antibody labeled with fluorescein. Figure 5 shows fluorescent micrographs of representative cells over a period of 24 h.

We used IPLab (Scientific Imaging Software) to quantitate the number, size, and spatial distribution of mature focal adhesions (FAs) in seven cells on each of the linear and cyclic RGD presenting SAMs 10 h after plating. All FAs having sizes greater than 0.14 μm^2 were considered mature and therefore counted. Cells on the cyclic RGD substrate had almost twice as many FAs (averaging 231 ± 30 FAs/cell) compared to cells on the linear RGD substrate (averaging 121 ± 49 FAs/cell). The size of FAs in cells on cyclic RGD was statistically smaller than on linear RGD, as shown by the probability curve in Figure 6. The median focal adhesion size for cells on cyclic RGD is 0.78 μm^2 and on linear RGD is 1.14 μm^2. The slope of the probability curve, which reflects the width of the distribution, was extracted by fitting the data to a sigmoidal function. FAs on the cyclic RGD have a narrower size distribution (slope = 0.43 ± 0.037) than FAs on the linear RGD (slope = 0.29 ± 0.016). We also observed differences in the spatial distribution of FAs in cells on the two substrates. On cyclic RGD, 38 ± 4% of the FAs were located in the interior of the cell (more than 10 μm from the perimeter), while on linear RGD, 28 ± 3% of the FAs were located in the interior of the cell. Hence, the ratio of FAs located on the cell perimeter relative to the interior is higher for substrates presenting linear RGD than for those presenting cyclic RGD peptide.

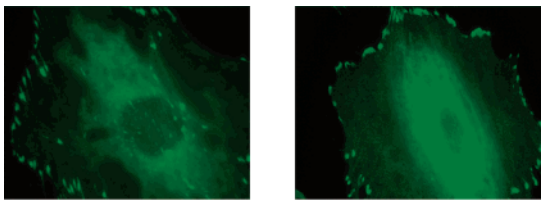

FIGURE 7: Formation of focal adhesions in cells on surfaces presenting either linear or cyclic RGD at 0.1% ligand density. The focal adhesions in cells on cyclic RGD at this lower density look similar to focal adhesions in cells on linear RGD, both in the reduced number of focal adhesions and in their distribution around the periphery of the cell.

We also briefly examined the effect of changing a second variable, ligand density affinity on focal adhesion formation (Figure 7). Focal adhesions in cells adhering to surfaces presenting the linear or cyclic RGD peptide at densities of 1% and 0.1% were examined. In comparison to cells on 1% cyclic RGD, cells on 0.1% cyclic RGD had fewer focal adhesions which were mainly located in the cell interior, resembling the pattern of focal adhesions on a surface presenting the linear RGD. The focal adhesions in cells on surfaces presenting the linear RGD were similar at both densities. This comparison shows that decreases in ligand density can counteract the effects of increases in ligand affinity. Further work will more completely address the role

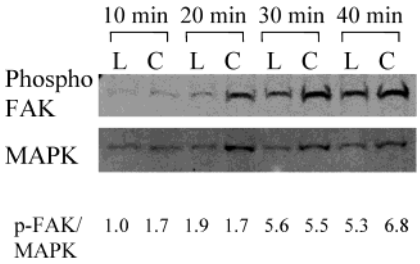

FIGURE 8: Western blotting to quantify the levels of phosphorylation of FAK in cells that were adherent to monolayers presenting either linear (L) or cyclic (C) RGD peptide. The top panel shows the Western blot probed with antibody against phosphorylated FAK at 10, 20, 30, and 40 min after plating. The lower panel shows the same Western blot that had been washed and then probed with antibody against MAP kinase to calibrate equal loading of protein. The bands were quantitated by Imagequant software (Molecular Dynamics), and the ratio of phospho-FAK to MAPK is presented below the gels. For cells on both linear and cyclic peptide, FAK was activated between 20 and 30 min after plating.

of ligand density in focal adhesion structure and the relative impact of affinity and density.

Focal Adhesion Signaling. We next characterized the onset of an integrin-mediated signal transduction pathway that results in phosphorylation of focal adhesion kinase (FAK) in order to determine whether the differences in focal adhesion structure within cells adherent to linear or cyclic RGD peptides had a consequence on a signaling pathway (*20*−*23*). Adherent cells on both model substrates were independently lysed at 10, 20, 30, or 40 min after plating. The cell lysate was separated on an electrophoresis gel, and the proteins were transferred to a nitrocellulose membrane and then stained with anti-phosphoFAK antibody. Western blotting, using mitogen-activated protein kinase (MAPK) as a calibration reference, showed that FAK is phosphorylated approximately 20 min after attachment for both high- and low-affinity surfaces (Figure 8).

DISCUSSION

Cell adhesion to the ECM is a critical process that is a key determinant for cell viability, proliferation, migration, and differentiation. Different substrata are known to have distinct effects on cell behavior. Cells remodel their environments by the secretion of ECM proteins and can therefore tailor their environments to promote specific cellular activities. To perceive these environmental changes, cells use transmembrane integrin receptors, which often aggregate with other integrin receptors and cellular proteins to further process this information. These aggregates, called focal adhesion complexes, are sites that bring together two important aspects of adhesion, mechanical links between the cell and the matrix and signal transduction, which are required to execute complex tasks such as spreading, migration, and gene regulation. The involvement of integrin receptors in both perceiving the environment and governing cell behavior suggests that the mechanism by which individual, ligand-bound receptors form aggregates is a key link to understanding how environmental factors affect cell response. In this study, we used chemically modified surfaces to completely control the extracellular environment in order to examine the mechanism by which affinity influences the organization of individual receptors into higher order structures.

The comparison of the adhesion of cells to surfaces presenting either a low-affinity or a high-affinity ligand for integrin receptors necessitated that the two substrates present peptide ligands at precisely the same density, since small changes in the density of the ligand can have dramatic effects on the attachment and spreading of cells (*9*). The customary method for preparing mixed monolayers relies on immersing the gold substrate in a solution of the peptide-terminated alkanethiol and glycol-terminated alkanethiol. This method has the limitation that the ratio of alkanethiolates in the monolayer is rarely identical to the ratio of alkanethiols in the solution. Further, because the relative amounts of the alkanethiolate in the monolayer depend on the structure of the terminal group, it is difficult to generate monolayers presenting either the linear or cyclic peptide at a constant density. To avoid this limitation, we prepared substrates by a quantitative Diels−Alder immobilization of peptide−diene conjugates to monolayers presenting quinone groups (Figure 1). This strategy ensured that the peptides were present at a uniform density across all substrates. Furthermore, the redox activity of the quinone permits the use of cyclic voltammetry to determine the density of this group in mixed SAMs (*24*, *25*).

Monolayers presenting RGD peptides are highly simplified mimics of ECM, yet our studies and others show that they replicate many functions of fibronectin-coated substrates (*26*−*28*). Cells attach to the model substrates by way of integrin receptors and spread to give a morphology that is characteristic of fibroblasts adherent to fibronectin. Cells adherent to the monolayers presenting peptide ligands have mature focal adhesions and organize actin stress filaments. Many integrin-initiated signaling pathways necessary for survival and division are active in cells adherent to these model substrates, and cells proliferate to a confluent population.

Inhibition experiments established that the differences in cell attachment to monolayers presenting either the linear or cyclic RGD peptide are due only to differences in the affinities of the ligand−receptor complex (Figure 4). While the soluble cyclic and linear RGD have been compared as inhibitors of cell adhesion, their affinities on surfaces as ligands have not been examined. The finding that the cyclic peptide reduced cell attachment by 50% at a concentration that was approximately 20-fold lower than was required with the linear peptide showed that the former has higher affinity for integrin receptors. These experiments also showed that the attachment of cells could be inhibited completely in all cases, demonstrating that cell attachment was mediated by the immobilized peptides alone. The finding that cyclic RGD could prevent cell attachment to monolayers presenting linear RGD further showed that the two ligands bind to the same set of integrin receptors. Previous studies have suggested that the cyclic peptide has a higher affinity for the $\alpha_v\beta_3$ over the $\alpha_5\beta_1$ integrin, while the linear peptide has no strong bias (*18*). While our results showed that both peptides bind to the same set of integrin receptors, they do not reveal whether the two peptides have different relative binding affinities for the two integrin receptors.

In this work, we varied the affinity of the integrin receptor for its ligand by using a conformationally restricted RGD peptide. The affinity of this interaction can also be influenced by changes in the receptor state. There is now substantial

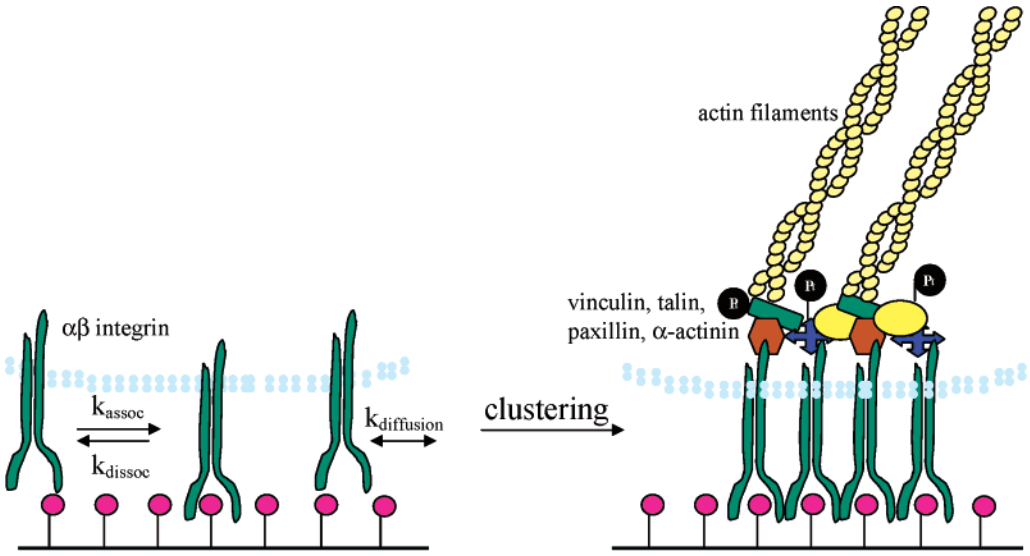

FIGURE 9: Model for receptor clustering into focal adhesions. The rate of receptor clustering depends on a number of factors including rates of association (k_{on}) and dissociation (k_{off}) of integrin binding to RGD, rate of diffusion in membrane ($k_{diffusion}$), ligand density, and receptor density. A dissociated receptor diffuses in the membrane where it can associate with a ligand in the proximity of other receptors to form clusters. Receptor engagement and clustering recruit intracellular proteins, which initiate integrin-mediated signaling and bind actin filaments.

evidence that cells can actively regulate the integrin receptors between low- and high-affinity states in a process known as inside-out regulation (*29*, *30*). We presume that the comparison of cells on linear and cyclic RGD peptides was not influenced by inside-out signaling since cell cultures were processed and maintained under identical conditions for the two substrates, and experiments were limited to short periods of time, but we cannot definitively rule out a differential level of integrin activation in cells attached to substrates presenting either high- or low-affinity ligands. In experiments where inside-out signaling is operative, we believe that the activation of integrins, to yield higher affinities for the immobilized ligands, will have an effect on focal adhesion structure that is similar to that demonstrated in this paper with high-affinity ligands.

Our finding that the efficiency of cell attachment, as determined by the number of cells that attached per unit area, was greater for substrates presenting the higher affinity ligand is consistent with findings in previous studies (*31*−*33*). Cell attachment to a surface requires a critical number of ligand−receptor interactions to form during transient contact of cell and surface. For ligand−receptor interactions that have a greater thermodynamic stability (larger binding affinity), fewer ligand−receptor interactions should be required to mediate the attachment; further, the larger association rate constant that applies to the higher affinity interaction should also result in a greater number of ligand−receptor interactions when the cell contacts the substrate.

The approach described in this paper introduces a model system that is well-suited for defining the biophysical mechanisms by which FAs assemble. Our study shows that changes in extracellular environment, ligand affinity in this case, indeed result in changes in the formation of focal adhesion complexes. Quantitative analysis of FAs showed that cells adherent to substrates presenting a high-affinity ligand have approximately 2-fold more FAs than do cells adherent by way of the low-affinity ligand and that these FAs are on average smaller in size. These results suggest that the assembly of focal adhesions is influenced by two rates: nucleation and growth of the FA. Our observations do not fit a simpler model involving one rate constant, in which case we would expect to see differences in the rate of formation but the same end pattern of focal adhesions.

We propose a mechanistic model that is consistent with our experimental results. We begin by recognizing that each polymerization event of receptors could be categorized into one of two processes: nucleation or growth. Nucleation describes the aggregation of two or more sets of mobile receptors into a cluster that does not dissociate. The cluster becomes irreversible because an intracellular network of proteins cross-links the integrin receptors together. This nucleated cluster can be considered stationary, since its diffusion is slow compared to other steps involved in polymerization. Growth describes the subsequent process of individual receptors (and smaller, mobile clusters) diffusing to the nucleated clusters. Our findings can be explained by considering the effect of affinity on the process of nucleation and growth of focal adhesions. On the cyclic RGD surface, nucleation occurs with higher frequency since the high-affinity interaction requires fewer receptors to form a stationary cluster. On the other hand, the growth of FAs on the cyclic RGD surface is slower as a result of the longer lifetime of the ligand−receptor complex (determined by a smaller k_{dissoc}) slowing down the effective diffusion rate of mobile receptors into the nucleated structures. We conclude that affinity affects the relative rates of nucleation to growth of FAs and as a result determines an outcome that favors either smaller, more numerous clusters or larger, less numerous clusters.

According to this model, a decrease in density would favor the growth of focal adhesions over nucleation due to faster receptor diffusion. We compared the formation of focal adhesions between cells adhering to surfaces presenting cyclic RGD at densities of 1% and 0.1% and, indeed, found the focal adhesions at the lower ligand density to be fewer in number and distributed largely in the periphery of the cell. The focal adhesions in cells adhering to linear RGD were similar for both densities. Our result that focal adhesion

formation on a surface presenting 0.1% cyclic RGD mimics focal adhesion formation on a surface presenting linear RGD indicates an overlap in the effect of these variables on focal adhesion formation.

Finally, we examined whether differences in distribution and size of focal adhesions in cells adherent by way of either high- or low-affinity ligands would result in different times in activation of downstream signaling pathways. In this work we characterized the activation of FAK because there is a direct correlation between receptor engagement and phosphorylation of FAK (*20*−*23*). We found that cells adherent to both model substrates showed phosphorylation of FAK within 20−30 min after plating. Because signaling of FAK occurs rapidly after initiation of cell spreading, finer differences in activation times cannot be determined from this assay. These results suggest that the initiation of FAK signaling and the rate of growth of this signal is approximately the same for both ligand affinities. However, this experiment does not determine whether maximal signaling at a later time point may differ due to differences in affinity.

A few previous studies have examined the adhesion of cells to model substrates presenting linear and cyclic RGD peptides. Xiao and Truskey found that bovine aortic endothelial cells were more adherent on siloxane monolayers presenting a cyclic RGD as compared to a linear RGD peptide (*31*). Kessler and co-workers have developed PMMA substrates that present cyclic RGD peptides to promote the α_v-dependent adhesion of osteoblasts for implant applications (*34*, *35*). More recently, Schense and Hubbell reported that the rate at which neurites migrated through fibrin matrices showed a biphasic dependence on the affinity of RGD ligands and that a lower concentration of cyclic peptide was required to support the maximum migration rate relative to that observed with the linear peptide (*32*). Taken together, these studies demonstrate the influence that ligand affinity has on cell adhesion and migration, but no studies have yet addressed the mechanistic aspects of receptor clustering that underlie these effects. On the basis of our observations that changes in affinity have opposite effects on the rate of nucleation and growth of FAs, we propose that the optimum affinity for a particular cell behavior strikes a balance between the extreme cases of strong ligand−receptor interactions that are completely individual and weak interactions that form a large aggregate. FAs may be the functional unit that is impacted by affinity, and this effect on the mechanical strength of adhesion may be sufficient to account for the changes in cell response.

The approach and studies described here for studying focal adhesion dynamics in adherent cells are very relevant to biological efforts to understand cell adhesion and migration. Recent reports have redefined focal adhesions as dynamic and motile structures within cells. Smilenov et al. imaged fibroblasts that were transfected with a GFP-tagged β_1 integrin and found that focal adhesions were motile in stationary cells but fixed in migrating cells (*36*). Other groups also imaged cells having GFP-tagged cytoskeletal proteins and found that focal adhesions were highly dynamic and underwent changes in protein composition as they translocated from the cell periphery to the interior (*37*, *38*). These reports underscore the need for mechanistic studies of the formation and dynamics of focal adhesions. This paper introduces such a study that used self-assembled monolayers presenting ligands and tri(ethylene glycol) groups as a model extracellular matrix to entirely control the ligand−receptor interactions that underlie cell adhesion. We believe that the model substrates described here, which can control the affinities, patterns, and even dynamic activities of immobilized ligands, will prove important for the types of mechanistic studies of cell adhesion described here and for characterizing the roles that peptide and carbohydrate ligands play in cell adhesion, migration, and differentiation (*24*, *25*, *39*, *40*).

ACKNOWLEDGMENT

We thank Shirley Bond of the Cancer Center Digital Light Microscopy Facility for assistance with fluorescent microscopy and image processing and Craig Lassy of the Confocal Digital Imaging Facility for assistance in using image analysis software.

REFERENCES

1. Boudreau, N., and Bissell, M. J. (1998) Extracellular matrix signaling: integration of form and function in normal and malignant cells, *Curr. Opin. Cell Biol. 10*, 640−646.
2. Buckley, C. D., Rainger, G. E., Bradfield, P. F., Nash, G. B., and Simmons, D. L. (1998) Cell adhesion: more than just glue, *Mol. Membr. Biol. 15*, 167−176.
3. Dedhar, S. (2000) Cell-substrate interactions and signaling through ILK, *Curr. Opin. Cell Biol. 12*, 250−256.
4. Curran, S., and Murray, G. I. (2000) Matrix metalloproteinases. Molecular aspects of their roles in tumour invasion and metastasis, *Eur. J. Cancer 36*, 1621−1630.
5. Ivaska, J., and Heino, J. (2000) Adhesion receptors and cell invasion: mechanisms of integrin-guided degradation of extracellular matrix, *Cell Mol. Life Sci. 20*, 16−24.
6. Mrksich, M. (2000) A surface chemistry approach to studying cell adhesion, *Chem. Soc. Rev. 29*, 267−273.
7. Roberts, C., Chen, C. S., Mrksich, M., Martichonok, V., Ingber, D. E., and Whitesides, G. M. (1998) Using mixed self-assembled monolayers presenting RGD and $(EG)_3OH$ groups to characterize long-term attachment of bovine capillary endothelial cells to surfaces, *J. Am. Chem. Soc. 120*, 6548−6555.
8. Ward, M. D., and Hammer, D. A. (1994) Focal contact assembly through cytoskeletal polymerization-steady-state analysis, *J. Math. Biol. 32*, 677−704.
9. Houseman, B. T., and Mrksich, M. (2000) Environment of Arg-Gly-Asp peptide ligands immobilized on self-assembled monolayers of alkanethiolates on gold influences the adhesion of 3T3 fibroblasts, *Biomaterials 22*, 943−955.
10. Mrksich, M., and Whitesides, G. M. (1997) Using self-assembled monolayers that present oligo(ethylene glycol) groups to control the interactions of proteins with surfaces, *ACS Symp. Ser. 680*, 361−373.
11. Prime, K. L., and Whitesides, G. M. (1991) Self-assembled organic monolayers−model systems for studying adsorption of proteins at surfaces, *Science 252*, 1164−1167.
12. Prime, K. L., and Whitesides, G. M. (1993) Adsorption of proteins onto surfaces containing end-attached oligo(ethylene oxide)−a model system using self-assembled monolayers, *J. Am. Chem. Soc. 115*, 10714−10721.
13. Mrksich, M., Sigal, G. B., and Whitesides, G. M. (1995) Surface-plasmon resonance permits in-situ measurement of protein adsorption on self-assembled monolayers of alkanethiolates on gold, *Langmuir 11*, 4383−4385.
14. Ulman, A. (1996) Formation and structure of self-assembled monolayers, *Chem. Rev. 96*, 1533−1554.
15. Dubois, L. H., and Nuzzo, R. G. (1992) Synthesis, structure, and properties of model organic surfaces, *Annu. Rev. Phys. Chem. 43*, 437−463.
16. Haubner, R. W., Schmitt, G., Holzemann, Goodman, S. L., Jonczyk, A., and Kessler, H. (1996) Cyclo RGD peptides containing beta-turn mimetics, *J. Am. Chem. Soc. 118*, 7881−7891.

17. Houseman, B. T., and Mrksich, M. (1998) An efficient solid-phase synthesis of peptide-substituted alkanethiols for the preparation of substrates that support cell adhesion, *J. Org. Chem. 63*, 7552−7555.
18. Haubner, R. R., Gratias, B., Diefenbach, S. L., Goodman, A., Jonczyk, and Kessler, H. (1996) Structural and functional aspects of RGD-containing cyclic pentapeptides as highly potent and selective integrin alpha(v)beta(3) antagonists, *J. Am. Chem. Soc. 118*, 7461−7472.
19. Yousaf, M. N., and Mrksich, M. (1999) Diels−Alder reaction for the selective immobilization of protein to electroactive self-assembled monolayers, *J. Am. Chem. Soc. 121*, 4286−4287.
20. Schense, J. C., and Hubbell, J. A. (2000) Three-dimensional migration of neurites is mediated by adhesion site density and affinity, *J. Biol. Chem. 275*, 6813−6818.
21. Kornberg, L., Earp, S. H., Parsons, J. T., Schaller, M., and Juliano, R. L. (1992) Cell adhesion or integrin clustering increases phosphorylation of a focal adhesion associated tyrosine kinase, *J. Biol. Chem. 267*, 23439−23442.
22. Hanks, S. K., Calalb, M. B., Harper, M. C., and Patel, S. K. (1992) Focal adhesion protein-tyrosine kinase phosphorylated in response to cell attachment to fibronectin, *Proc. Natl. Acad. Sci. U.S.A. 89*, 8487−8491.
23. Parsons, J. T. (2003) Focal adhesion kinase: the first ten years, *J. Cell Sci. 116*, 1409−1416.
24. Yousaf, M. N., Houseman, B. T., and Mrksich, M. (2001) Turning on cell growth with electroactive substrates, *Angew. Chem., Int. Ed. 40*, 1093−1096.
25. Yousaf, M. N., Houseman, B. T., and Mrksich, M. (2001) Using electroactive substrates to pattern the attachment of two different cell types, *Proc. Natl. Acad. Sci. U.S.A. 98*, 5992−5996.
26. Burridge, K., Turner, C. E., and Romer, L. H. (1992) Tyrosine phosphorylation of paxillin and pp125 (FAK) accompanies cell-adhesion to extracellular-matrix—a role in cytoskeletal assembly, *J. Cell Biol. 119*, 893−903.
27. Kim, J. P., Zhang, K., Chen, J. D., Wynn, K. C., Kramer, R. H., and Woodley, D. T. (1992) Mechanism of human keratinocyte migration on fibronectin—unique roles of RGD site and integrins, *J. Cell. Physiol. 151*, 443−450.
28. Massia, S. P., and Hubbell, J. A. (1991) An RGD spacing of 440 nm is sufficient for integrin $\alpha_v\beta_3$-mediated fibroblast spreading and 140 nm for focal contact and stress fiber formation, *J. Cell Biol. 114*, 1089−1100.
29. Kim, M., Carman, C. V., and Springer, T. A. (2003) Bidirectional transmembrane signaling by cytoplasmic domain separation in integrins, *Science 301*, 1720−1725.
30. Liddington, R. C., and Ginsberg, M. H. (2002) Integrin activation takes shape, *J. Cell Biol. 158*, 833−839.
31. Xiao, Y., and Truskey, G. A. (1996) Effect of receptor−ligand affinity on the strength of endothelial cell adhesion, *Biophys. J. 71*, 2869−2884.
32. Schlaepfer, D. D., and Hunter, T. (1998) Integrin signaling and tyrosine phosphorylation: just the FAKs?, *Trends Cell Biol. 8*, 151−157.
33. Kuo, S. C., and Lauffenburger, D. A. (1993) Relationship between receptor/ligand binding affinity and adhesion strength, *Biophys. J. 65*, 2191−2200.
34. Kantlehner, M., Finsinger, D., Meyer, J., Schaffner, P., Jonczyk, A., Diefenbach, B., Nies, B., and Kessler, H. (1999) Selective RGD-mediated adhesion of osteoblasts at surfaces of implants, *Angew. Chem., Int. Ed. 38*, 560−562.
35. Kantlehner, M., Schaffner, P., Finsinger, D., Meyer, J., Jonczyk, A., Diefenbach, B., Nies, B., Holzemann, G., Goodman, S. L., and Kessler, H. (2000) Surface coating with cyclic RGD peptides stimulates osteoblast adhesion and proliferation as well as bone formation, *ChemBioChem 1*, 107−114.
36. Smilenov, L. B., Mikhailov, A., Pelham, R. J., Marcantonio, E. E., and Gundersen, G. G. (1999) Focal adhesion motility revealed in stationary fibroblasts, *Science 286*, 1172−1174.
37. Laukaitis, C. M., Webb, D. J., Donais, K., and Horwitz, A. F. (2001) Differential dynamics of α5 integrin, paxillin, and α-actinin during formation and disassembly of adhesions in migrating cells, *J. Cell Biol. 153*, 1427−1440.
38. Zamir, E., Katz, M., Posen, Y., Erez, N., Yamada, K. M., Katz, B. Z., Lin, S., Lin, D. C., Bershadsky, A., Kam, Z., and Geiger, B. (2000) Dynamics and segregation of cell−matrix adhesions in cultured fibroblasts, *Nat. Cell Biol. 2*, 191−196.
39. Hodneland, C. D., and Mrksich, M. (2000) Biomolecular surfaces that release ligands under electrochemical control, *J. Am. Chem. Soc. 122*, 4235−4236.
40. Yeo, W. S., Hodneland, C. D., and Mrksich, M. (2000) Electroactive monolayer substrates that selectively release adherent cells, *ChemBioChem. 2*, 590−593.

BI0352670